Cardiac MicroRNA Expression Profile After Experimental Brain Death Is Associated With Myocardial Dysfunction and Can Be Modulated by Hypertonic Saline

Ludmila Rodrigues Pinto Ferreira, PhD,[1,2] Cristiano Jesus Correia, PhD,[3] Fernando Luiz Zanoni, PhD,[3] Ana Carolina Carvalho-Silva, MSc,[1,2] Ricardo Zaniratto, BSc,[4,5] Darlan da Silva Cândido, MSc,[4,5] Rafael Ribeiro Almeida, PhD,[4,5] Ana Cristina Breithaupt-Faloppa, PhD,[3] Edecio Cunha-Neto, MD, PhD,[4,5,6] and Luiz Felipe P. Moreira, MD, PhD[3]

Background. Brain death (BD) is associated with systemic inflammatory compromise, which might affect the quality of the transplanted organs. This study investigated the expression profile of cardiac microRNAs (miRNAs) after BD, and their relationship with the observed decline in myocardial function and with the changes induced by hypertonic saline solution (HSS) treatment. **Methods.** Wistar rats were assigned to sham-operation (SHAM) or submitted to BD with and without the administration of HSS. Cardiac function was assessed for 6 h with left ventricular (LV) pressure-volume analysis. We screened 641 rodent miRNAs to identify differentially expressed miRNAs in the heart, and computational and functional analyses were performed to compare the differentially expressed miRNAs and find their putative targets and their related enriched canonical pathways. **Results.** An enhanced expression in canonical pathways related to inflammation and myocardial apoptosis was observed in BD induced group, with 2 miRNAs, miR-30a-3p, and miR-467f, correlating with the level of LV dysfunction observed after BD. Conversely, HSS treated after BD and SHAM groups showed similar enriched pathways related to the maintenance of heart homeostasis regulation, in agreement with the observation that both groups did not have significant changes in LV function. **Conclusions.** These findings highlight the potential of miRNAs as biomarkers for assessing damage in BD donor hearts and to monitor the changes induced by therapeutic measures like HSS, opening a perspective to improve graft quality and to better understand the pathophysiology of BD. The possible relation of BD-induced miRNA's on early and late cardiac allograft function must be investigated.

(*Transplantation* 2022;106: 289–298).

Received 9 December 2020. Revision received 8 February 2021.

Accepted 9 March 2021.

[1] RNA Systems Biology Laboratory (RSBL), Departamento de Morfologia, Instituto de Ciências Biológicas, Universidade Federal de Minas Gerais, Belo Horizonte, Minas Gerais, Brazil.

[2] National Institute of Science and Technology for Vaccines (INCTV), Belo Horizonte, Minas Gerais, Brazil.

[3] Laboratório Cirúrgico de Pesquisa Cardiovascular (LIM-11), Instituto do Coração (InCor), Hospital das Clínicas HCFMUSP, Faculdade de Medicina, Universidade de São Paulo, São Paulo, Brazil.

[4] Laboratório de Imunologia, Instituto do Coração (InCor), Hospital das Clínicas HCFMUSP, Faculdade de Medicina, Universidade de São Paulo, São Paulo, Brazil.

[5] Institute for Investigation in Immunology (INCT-iii), São Paulo, Brazil.

[6] Laboratório de Imunologia Clínica e Alergia, Faculdade de Medicina, Universidade de São Paulo, São Paulo, Brazil.

L.R.P.F. and C.J.C. are cofirst authors and contributed equally to this work.

L.R.P.F. and C.J.C. performed the study, analyzed data, and wrote the article. F.L.Z., A.C.C.S., R.Z., D.d.S.C., and R.R.A. contributed to obtaining and analyzing data. A.C.B.-F. analyzed data and wrote the article. E.C.-N. and L.F.P.M. designed the study, contributed to analyzing data, and wrote the article.

The authors declare no conflicts of interest.

*This work was supported by Fundação de Amparo à Pesquisa do Estado de São Paulo "FAPESP" (grants numbers 2012/19841-2, 2013/50302-3, 2014/50890-5). L.R.P.F. had financial support from Brazilian National Institute of Science and Technology for Vaccines (INCT/CNPq) and Programa Institucional de Auxílio à Pesquisa de Docentes Recém-Contratados pela UFMG PRPq Edital 09/2019—projeto 27764*76.*

The data that support the findings of this article are available within the article [and] its supplementary materials http://links.lww.com/TP/C209. and from the corresponding authors upon reasonable request.

Supplemental Visual Abstract; http://links.lww.com/TP/C210.

Supplemental digital content (SDC) is available for this article. Direct URL citations appear in the printed text, and links to the digital files are provided in the HTML text of this article on the journal's Web site (www.transplantjournal.com).

Correspondence: Luiz Felipe P. Moreira, MD, PhD, Laboratório Cirúrgico de Pesquisa Cardiovascular (LIM-11), Instituto do Coração (Incor), Hospital das Clínicas HCFMUSP, Av. Dr. Enéas Carvalho de Aguiar, 44, São Paulo, SP, Brazil 05403-000. (luiz.moreira@incor.usp.br); Edecio Cunha-Neto, MD, PhD, Laboratório de Imunologia, Instituto do Coração (InCor), Hospital das Clínicas HCFMUSP, Av. Dr. Enéas Carvalho de Aguiar, 44, São Paulo, SP, Brazil 05403-000. (edecunha@gmail.com).

ISSN: 0041-1337/20/1062-289

DOI: 10.1097/TP.0000000000003779

<zdoi;10.1097/TP.0000000000003779>

INTRODUCTION

Heart transplantation continues to be the treatment of choice for end-stage heart failure. The number of patients on waiting lists, however, is much higher than the number of available organs. Brain death (BD) donors are the most important source of organs for heart transplantation; however, BD is associated with myocardial dysfunction, severe hemodynamic changes, and systemic inflammatory compromise, which might affect the quality of the transplanted organs.[1-3] Although mechanisms responsible for this dysfunction remain poorly understood, several authors have demonstrated the involvement of apoptotic and inflammatory pathways in donor heart deterioration.[2,4,5]

MicroRNAs (miRNA) are noncoding RNA molecules that regulate gene expression posttranscriptionally by modulating protein expression in different pathways. It has been shown that miRNAs participate in various physiologic homeostatic processes and their dysregulated expression is induced in several cardiovascular disorders.[6-8] Understanding the role of these molecules in the pathogenesis of myocardial dysfunction induced by BD could permit improved outcomes of marginal grafts and the use of formerly unusable donor hearts.

We have previously published that the use of hypertonic saline solution (HSS) ameliorates left ventricular dysfunction and seems to improve myocardial tissue deterioration, reducing inflammatory changes and apoptosis after BD induction in rats.[9] In the same experimental setup, we now investigated the global expression profile of cardiac miRNAs after BD and their relationship with the observed decline in myocardial function. We also sought to examine whether the amelioration of functional parameters with HSS was associated with an altered miRNA expression profile. Further, we identified an enrichment in canonical pathways potentially regulated by the differentially expressed miRNAs.

MATERIALS AND METHODS

Ethics Statement

The protocols were approved by the Animal Subject Committee of Sao Paulo University Medical School with the number 346/12. All experiments were performed in accordance with the ethical principles for animal research adopted by the Brazilian College of Animal Experimentation, and the animals received humane care in compliance with the 2011 "Guide for the Care and Use of Laboratory Animals," recommended by the US National Institutes of Health.

Groups and Treatment

Fifteen male Wistar rats weighing 250–300 g were used in experimental protocols. Rats were randomly divided into 3 groups of 5 animals: (1) SHAM—rats that were subjected to surgical procedures without BD induction; (2) BD—rats that were treated with normal saline solution (NaCl 0.9%, 4 mL/kg) injected intravenously immediately after BD induction; (3) HSS—rats that were treated with HSS (NaCl 7.5%, 4 mL/kg) injected intravenously as a bolus 60 min after BD was initiated. All animals were evaluated for 6 h.

Brain Death Induction Model

All animals were initially anesthetized with 5% isoflurane. The anesthesia was maintained with 2% isoflurane inhalation, and animals were kept mechanically ventilated (rodent ventilator-Harvard Apparatus, model 683) until BD induction and during the entire experiment for the SHAM group. BD was induced by rapid inflation of a catheter Fogarty-4F (Baxter Health Care Co, United States) with 0.5 mL of saline solution through a drilled parietal burr hole. It was confirmed by maximal pupil dilatation, apnea, absence of reflex, and drop of mean arterial pressure.[9] Animals from the SHAM group were trepanned only.

Hemodynamic Measurements

In all groups, a 2-F microtip pressure-volume conductance catheter (SPR-838 AD Instruments Inc., Colorado Springs, CO) was inserted into the right carotid artery and advanced into the left ventricle to assess cardiac function during a 6-h period. Hemodynamic parameters were calculated using an acquisition system (MPVS, AD Instruments Inc.) coupled to pressure-volume analysis software (LabChart 8, AD Instruments Inc.). Data were obtained for the following left ventricular (LV) parameters: ejection fraction, stroke work, and pressure-volume loop. LV myocardial contraction efficiency was estimated via the ratio between LV stroke work and pressure-volume area.

MiRNA Sample Preparation

Hearts were procured at the end of the experimental procedure. Ventricular samples collected from the left ventricular wall from each heart were immersed in 500 µL of lysis buffer from mirVana miRNA Isolation Kit (Ambion, USA) and mechanically disrupted with the Precellys 24-bead-based homogenizer (Bertin Technologies, France). Total RNA enriched in miRNAs was isolated according to the manufacturer's protocol. RNA concentration and purity were measured using a NanoDrop-1000 spectrophotometer (Thermo Scientific, USA), and the integrity was determined on a Bioanalyzer 2100 (Agilent, USA). Only samples with total RNA RIN (RNA Integrity Number) value >8.0 were used in our analyses.

MiRNA Expression Profiling

Cardiac miRNA expression profiling was performed in 5 rats per group, and a total of 641 miRNAs were screened according to Thermo Fisher protocols. Briefly, we used a multiplexed RT reaction (*Megaplex* RT stem-loop primers, Rodent Pool Set v3.0 kit) to produce cDNA from 500 ng isolated total RNA. The obtained cDNA sample and Real time-PCR master mix (TaqMan Universal Master Mix II, no UNG-Thermo Fisher) were loaded into preprinted TaqMan Low Density Arrays (TLDA) microfluidic cards (Rodent Card A + B v3, format 384 wells each). The real time–PCR reaction was performed on a *QuantStudio* 12K Flex Real-Time PCR System (Applied Biosystems, USA).

Unsupervised Analysis of miRNA Expression

To analyze the differences in miRNA expression levels between the 3 groups, we uploaded the real-time generated raw data files in a ThermoFisher Cloud software v1.0 (Connect, https://www.thermofisher.com/br/en/home/cloud.html). The data files were first preprocessed using automatic

baseline corrections and manually checked for each assay if the threshold cycle (Ct) value corresponded to the midpoint of the logarithmic amplification curve. MiRNAs with a mean Ct >36 and detected in <80% of all samples were considered below the detection level and excluded from further analysis. The comparative threshold cycle method was used to calculate the relative miRNA expression levels (ΔCt) after global mean normalization. The miRNAs with threshold values of $P \leq 0.05$ and absolute fold change (FC) ≥1.5 were considered differentially expressed.

DEMs Target Prediction, Functional Enrichment Analysis

MiRNA target prediction, canonical pathways analysis, network construction, and upstream regulator analysis were performed using Ingenuity Pathway Analysis software (IPA, Qiagen). First, we used the IPA target filter tool to identify potential targets of the list of differentially expressed miRNAs (DEMs) identified in each group. We only considered as potential targets, the ones which were experimentally validated, and computationally predicted targets based on the content of the 2020–07 release, incorporating 3 algorithms (*TargetScan*, *TarBase*, and *miRecords*). IPA was also used to identify significantly enriched canonical pathways within the list of DEMs and their potential identified targets.

Statistical Analysis

Data were analyzed using GraphPad Prism 8.2 software (GraphPad Software Inc., La Jolla, CA). Differences between groups were analyzed using the Kruskal-Wallis test followed by Dunn's test for multiple comparisons, or 2-way ANOVA followed by Bonferroni tests for multiple comparisons after rank transformation of the absolute values. Correlation coefficients were calculated by the Pearson method. Results are expressed as median and interquartile variation.

RESULTS

There were no deaths, and all animals completed the designed study protocol. Figure 1 is a flow diagram

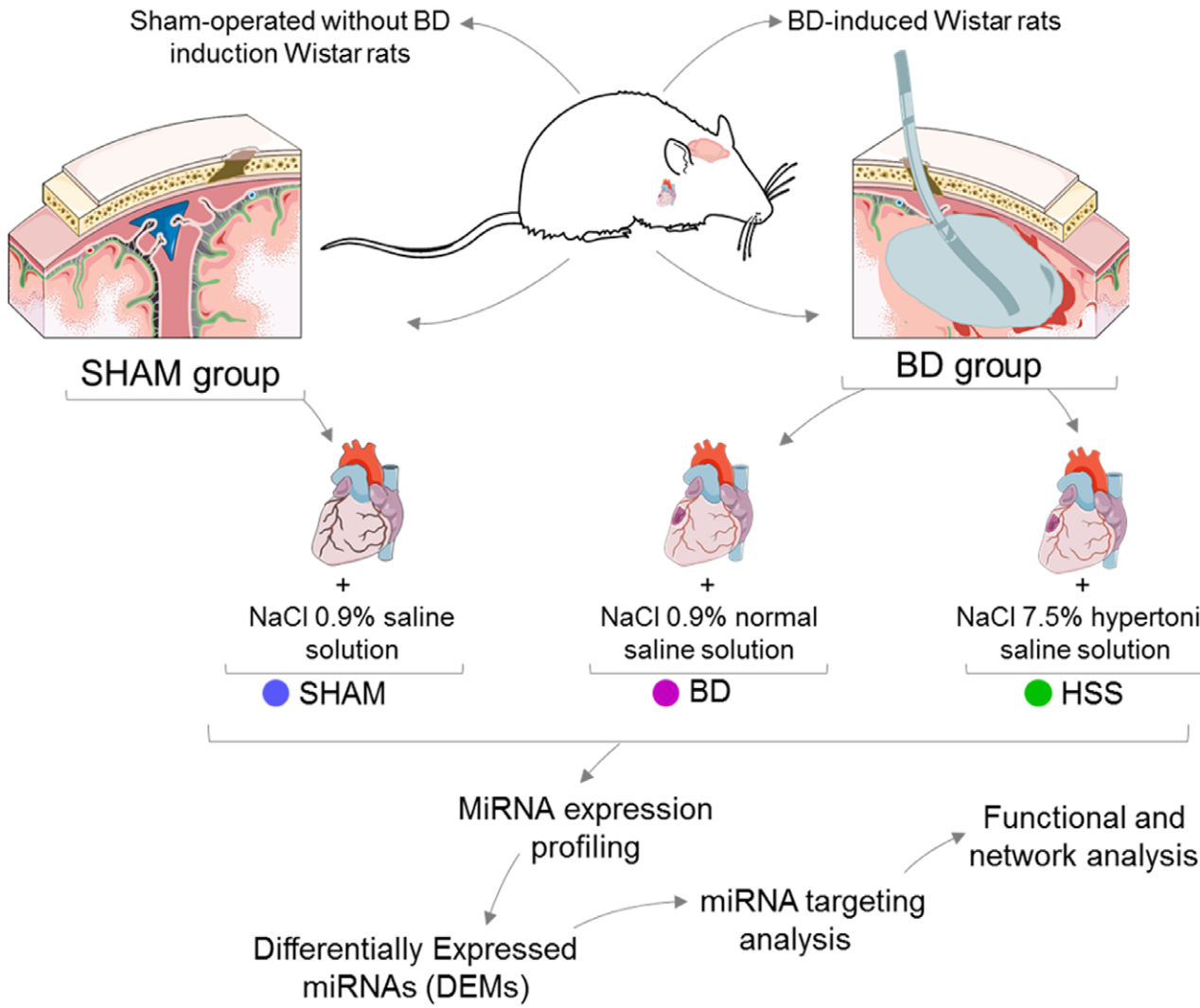

FIGURE 1. Workflow of experimental BD induction procedure, data processing, and analysis of miRNA expression profiles. Wistar rats were BD induced, and SHAM operated without BD induction (blue). The BD induced group was divided in subgroups: BD (treated with NaCl 0.9% normal saline solution) (magenta) and HSS (treated with NaCl 7.5% hypertonic saline solution—HSS) (green). After 6 h of BD induction, the hearts of the rats were procured and keep at –80 ºC until RNA isolation. miRNA expression profiling was performed for all 3 groups, and DEMs were identified for each comparison. With the lists of DEMs, we performed miRNA targeting and functional analysis. BD, brain death; DEM, differentially expressed miRNA; HSS, hypertonic saline solution; miRNA, microRNA; SHAM, sham-operation.

depicting the procedural steps and division of the experimental groups. Total volume of fluid administered during the experiments was similar between the groups. No differences were observed in blood gases, cell counts, or basal electrolyte levels (data not shown). Table 1 shows that hemodynamic parameters were similar in all groups at baseline. Left ventricle (LV) ejection fraction and stroke work were decreased after 6 h in BD group in comparison to SHAM experiments, while they were improved under HSS treatment in relation to BD group. Figure 2 shows the variation in myocardial contraction efficiency in the 3 groups. After 6 h of experimentation, this parameter was significantly reduced in the BD group compared with SHAM experiments. However, the observed values of myocardial contraction efficiency with HSS treatment were similar to SHAM group.

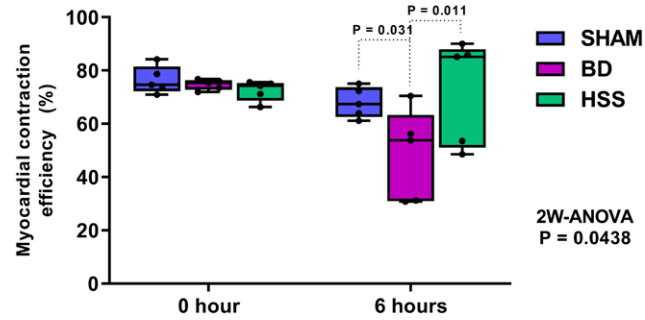

FIGURE 2. Myocardial contraction efficiency before and 6 h after brain death induction. The groups are SHAM, BD, and brain death with HSS treatment. Each measurement is shown as a black dot. The upper and lower borders of the boxes represent the upper and lower quartiles. The middle horizontal line is the median value. ANOVA, analysis of variance; BD, brain death; HSS, hypertonic saline solution; SHAM, sham-operation

Identification of Differentially Expressed miRNAs and Their Potential Targets

Figure 3 shows volcano plots of –log 10 (*P*) versus the log 2 of FC values for each miRNA. The analysis revealed a total of 30 DEMs (20 downregulated and 10 upregulated) between BD and SHAM (Figure 3A). The comparison between HSS and BD showed 31 DEMs (14 downregulated and 17 upregulated) (Figure 3B), whereas that between HSS and SHAM demonstrated a total of 19 DEMs (13 downregulated and 6 upregulated) (Figure 3C).

From the list of 30 DEMs identified on BD versus SHAM comparison, we obtained information of 12 miRNAs targeting 373 mRNAs, considering only experimentally validated targets. Further, from the list of 31 DEMs identified on HSS versus BD and 19 from the HSS versus SHAM comparisons, we obtained targeting information for 20 and 13 DEMs, respectively. The lists of DEM targets are depicted in **Table S1, SDC**, http://links.lww.com/TP/C209.

DEMs Targets Set Enrichment Analysis and Identification of Canonical Pathways

For this analysis, we only considered experimentally validated targets within the list of targets for each comparison: BD versus SHAM, HSS versus BD, and HSS versus SHAM. Figure 4A–C shows the top 25 canonical pathways among the most enriched pathways for the DEMs targets found in each comparison listed on **Table S2, SDC**, http://links.lww.com/TP/C209. The graphs display the percentage of DEMs present in each pathway with the total number of molecules of the given pathway displayed in the top of the bars. We observed an over-representation of canonical pathways related to inflammation and immune response and, most importantly, pathways related to cardiac hypertrophy signaling and apoptosis for the BD versus SHAM comparison (Figure 4A). In contrast, we observed that nearly all inflammatory pathways over-represented in the BD versus SHAM comparison were absent in the comparisons of HSS versus BD or SHAM groups (Figure 4B,C). In the latter 2 comparisons, we also found over-representation of many signaling and regulatory pathways of growth factors and proteins related to cell proliferation, integrity maintenance, and survival. In Figure 5, the DEMs relative expression can be observed for 9 miRNAs that were either up or downregulated after BD in relation to the SHAM group and had their relative expression reversed to similar values to the SHAM group after the infusion of HSS.

Correlation of Expression Profiles of miR-467F and miR-30a-3p With Myocardial Contraction Efficiency

To further identify DEMs that might be indirectly associated with cardiac alterations after BD, we performed a correlation analysis with the percentage decrease in myocardial contraction efficiency observed 6 h after BD induction and the miRNA expression level of the DEMs observed in the BD versus SHAM comparison. The expression profiles of miR-467f and miR-30a-3p were found to be significantly correlated with the percentage decrease in

TABLE 1.

Left ventricular hemodynamic parameters before and 6 h after brain death induction

	SHAM		BD		HSS	
	0 h	6 h	0 h	6 h	0 h	6 h
LV ejection fraction (%)	66.4 (62.8–72.8)	59.3 (44.1–59.3)[a]	62.7 (56.1–66.9)	46.7 (23.1–55.3)[a,b]	64.3 (54.1–70.3)	63.4 (48.1–76.2)[b]
LV stroke work (mm Hg * mL)	13.0 (10.5–15.5)	14.5 (10.1–16.2)	12.5 (11.5–13.4)	9.5 (2.4–15.7)[c]	12.8 (11.2–20.7)	12.3 (7.3–29.5)[c]
LV pressure-volume area (mm Hg * mL)	16.9 (15.5 – 19.6)	21.1 (18.2–25.3)	16.5 (15.5–17.6)	14.6 (7.8–20.0)	17.2 (14.8–20.9)	17.3 (12.5–28.3)

The groups are SHAM, BD, and brain death with HSS treatment. Data are presented as median and lower to upper limits.
[a]HHS vs BD at 6 h $P = 0.041$
[b]HSS vs BD at 6 h $P = 0.005$
[c]BD vs SHAM at 6 h $P = 0.047$.
BD, brain death; HSS; hypertonic saline solution; LV, left ventricular, SHAM, sham-operation.

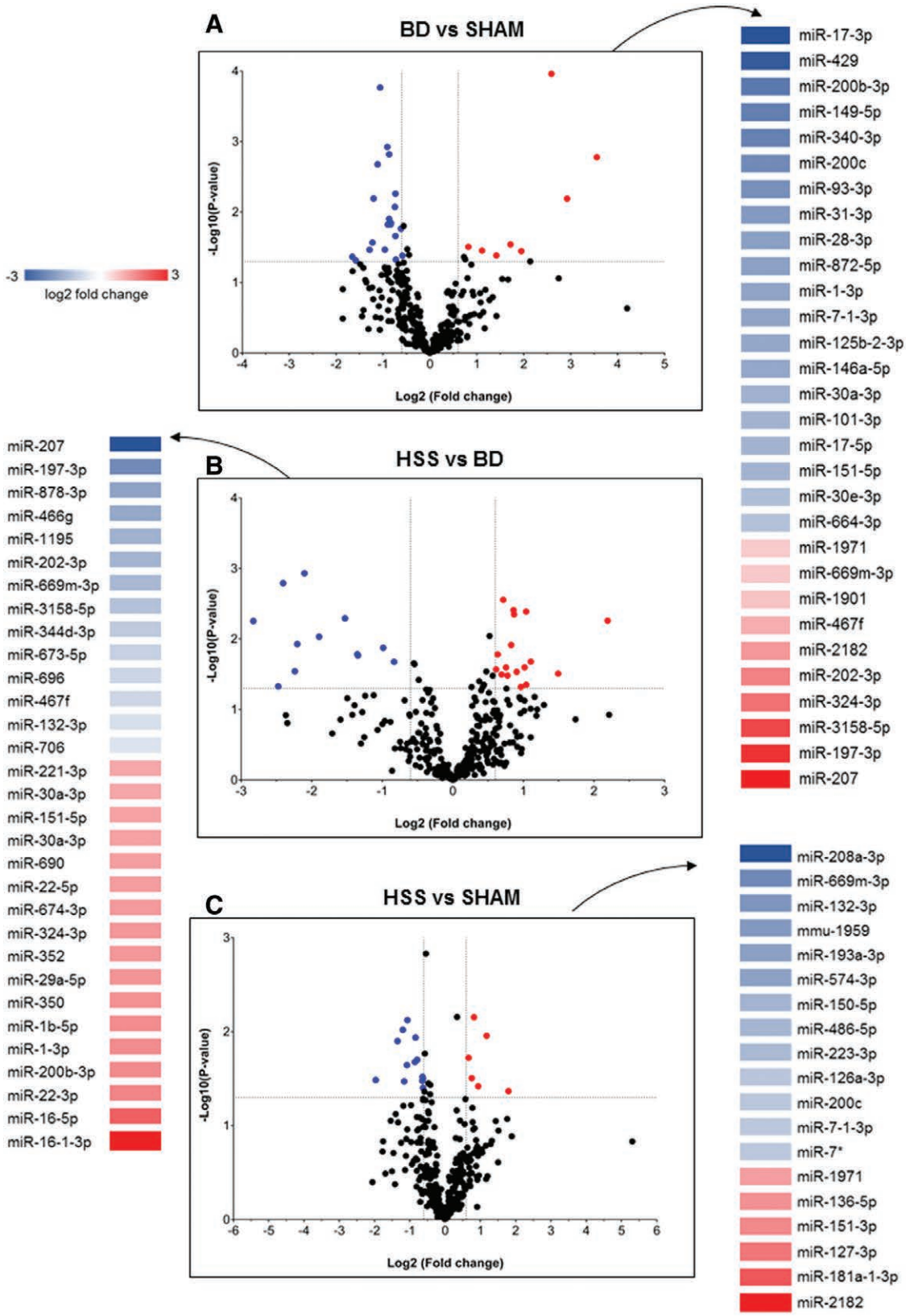

FIGURE 3. Differentially expressed miRNAs after BD induction and HSS treatment. Volcano plots representation for each comparison (A) BD vs SHAM, (B) HSS vs BD, and (C) HSS vs SHAM. The volcano plots of –log 10 (*P*) vs the log 2-FC values for each miRNA. The red and blue dots indicate miRNAs significantly (FDR adjusted $P < 0.05$) upregulated and downregulated (with 1.5 of FC cutoff), respectively. The list of DEMs are represented as heatmaps also with graduations of blue (downregulated) to red (upregulated) based on the log 2 transformed FC values. The analysis revealed a total of 30 DEMs (20 downregulated and 10 upregulated) between BD and SHAM. The comparison between HSS and BD showed 31 DEMs (14 downregulated and 17 upregulated), whereas that between HSS and SHAM demonstrated a total of 19 DEMs (13 downregulated and 6 upregulated). BD, brain death; DEMs, differentially expressed miRNA; FC, fold change; FDR, false discovery rate; HSS, hypertonic saline solution; miRNA, microRNA; SHAM, sham-operation.

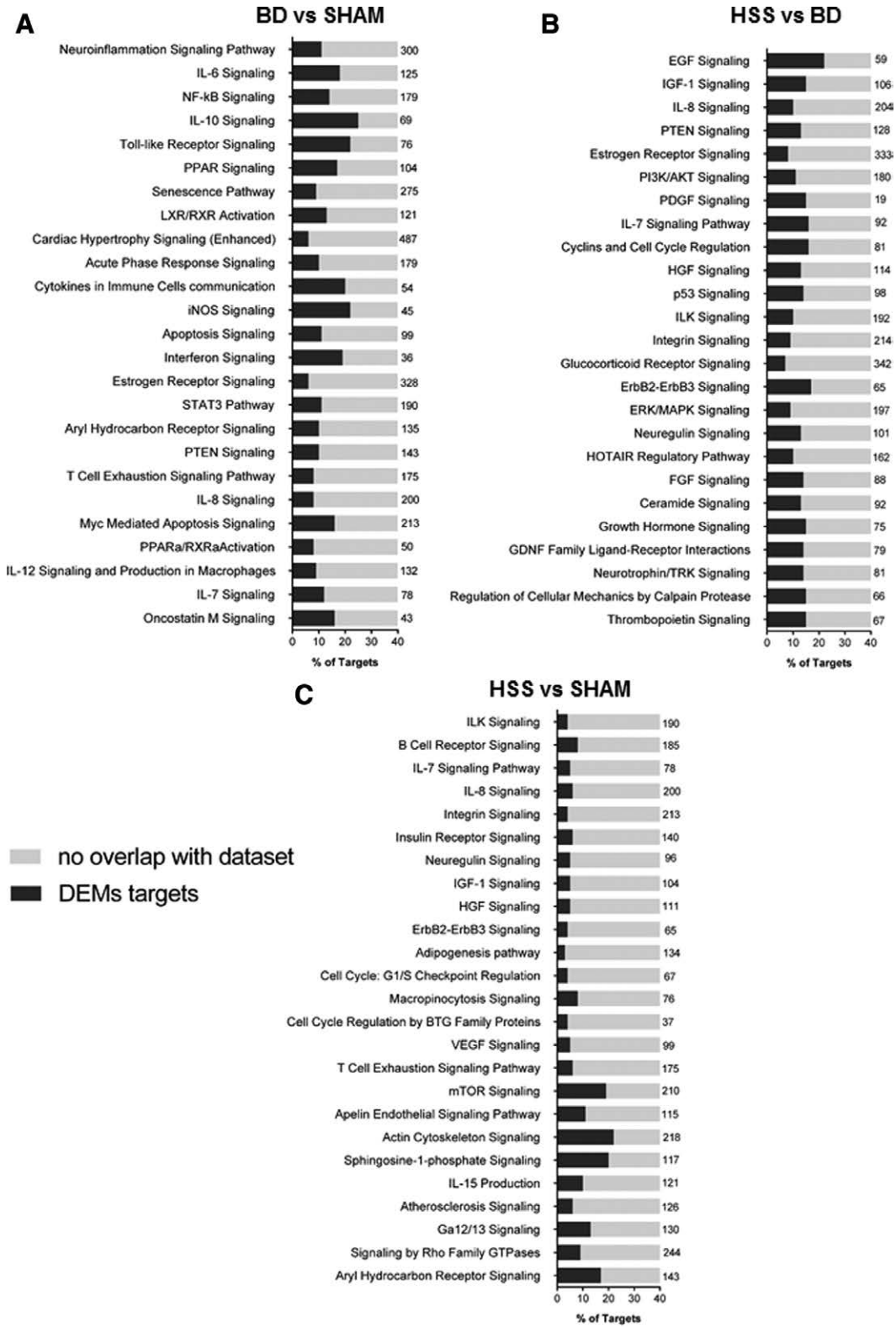

FIGURE 4. Functional pathways enriched after BD induction and HSS treatment. The stacked bar charts display the percentage of DEMs targets within the top 25 canonical pathways most enriched in each comparison: (A) BD vs SHAM, (B) HSS vs BD, and (C) HSS vs SHAM. The numbers in the top of each bar represent the total number of molecules in the specific listed pathway. BD, brain death; BTG, B-cell translocation gene; DEM, differentially expressed miRNA; EGF, epidermal growth factor; ErbB2-ErbB3, receptor tyrosine-protein kinase 2-3; ERK/MAPK, extracellular-signal-regulated kinase/mitogen-activated protein kinase; FGF, fibroblast growth factor; Ga 12/13, guanine nucleotide-binding proteins subunit alpha-12/13; GDNF, glial cell-derived neurotrophic factor; GTPases, GDP enzymes; HGF, hepatocyte growth factor; HSS, hypertonic saline solution; IGF-1, recombinant human insulin-like growth factor 1; IL, interleukin; ILK, Integrin-linked kinase; iNOS, inducible nitric oxide synthase; LXR/RXR, liver X receptor/retinoid X receptor; miRNA, microRNA; NF, nuclear factor; PDGF, platelet-derived growth factor; PI3K/AKT, phosphoinositide/protein kinase B; PTEN, phosphatase and tensin homolog deleted on chromosome 10; SHAM, sham-operation; STAT3, signal transducer and activator of transcription 3; VEGF, vascular endothelial growth factor.

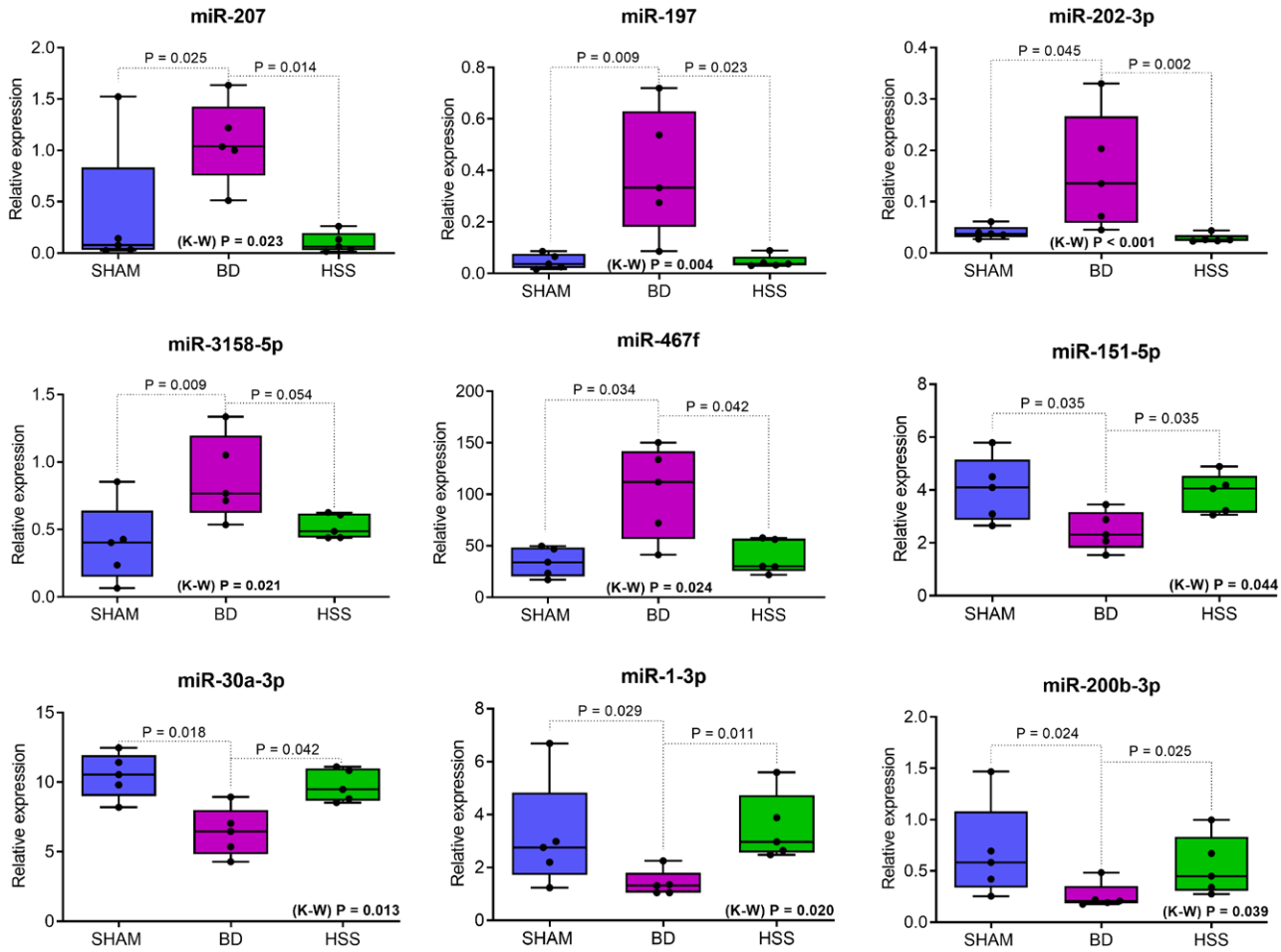

FIGURE 5. Relative expression of 9 differentially expressed miRNAs in the 3 studied groups. The miRNAs were up regulated or downregulated after BD induction in relation to SHAM experiments and in opposite situation after HSS infusion in relation to BD group without treatment. Each measurement is shown as a black dot. The upper and lower borders of the boxes represent the upper and lower quartiles. The middle horizontal line is the median value. BD, brain death; HSS, hypertonic saline solution; K-W, Kruskal-Wallis test; miRNA, microRNA; SHAM, sham-operation.

myocardial contraction efficiency (Figure 6). Looking for the key pathways and molecules related to heart pathophysiology, we identified *Cardiac β-adrenergic* and *Protein Kinase A signaling* among the enriched pathways known as potentially regulated by miR-487f (Figure 7A). For miR-30a-3p (Figure 7B), we observed enrichment in pathways related to the regulation of cardiomyocyte contractility and function: *Adrenomedullin* and *Paxillin signaling pathways*.

DISCUSSION

Some studies discuss the use of miRNAs as biomarkers of organ quality[10,11] and as new players associated with early and late allograft dysfunctions,[12-14] but there is not enough information regarding their role in heart grafts obtained from BD donors. Herein, we identified miRNAs that potentially regulate key pathways involving cardiac pathophysiological changes and hemodynamic behavior after BD induction in a rodent model. Moreover, we observed that HSS treatment induced the reversion of the altered expression of several miRNAs and the modulation of pathogenic pathways that were modified in the heart graft after BD, in accordance with the previously published data regarding the cellular inflammatory and apoptotic changes documented in the same experimental model.[9]

The signaling and regulatory pathways associated with BD induction identified in the heart and reversed here after HSS treatment were mainly related to inflammatory changes and myocardial apoptosis, factors that have been related to donor myocardial dysfunction.[4,5,9] Cardiomyocyte survival was previously described as regulated by several miRNAs that work by suppressing/inhibiting the expression of proapoptotic molecules.[6,15] From the 30 dysregulated miRNAs after BD observed here, several appear to be involved in promoting the apoptotic process. This involvement was probably dictated by alterations related to the downregulation of miR-17-3p, miR-149-5p, miR-93-3p, miR-1-3p, miR-125b-5p, miR-146a-5p, and miR-30a-3p, and the upregulation of miR-197-3p, miR-207, and miR-467f. Besides other contributions, downregulation of the mir-30 family is correlated with alterations in *cardiac beta-adrenergic signaling* by enhancing apoptosis.[6,15] Conversely, the reversion of lower levels of miR-30a-3p has the effect of reducing cell apoptosis by the regulation of the *phosphatase and tensin homolog deleted on chromosome 10 (PTEN)/phosphoinositide (PI3K)/protein kinase B (AKT) pathway*.[16] Furthermore, overexpression of adrenomedullin and paxillin associated with miR-30a-3p seems to protect cells against hypoxia and apoptosis via the *AKT and BCL-2 signaling pathways*.[17,18]

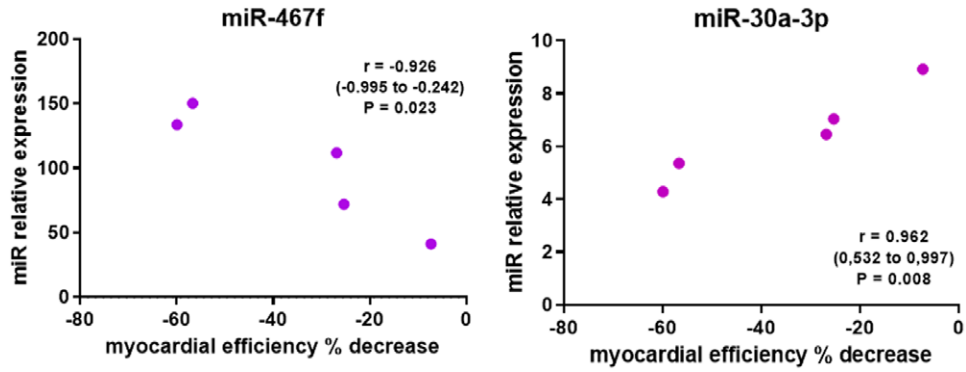

FIGURE 6. Correlation between the relative expression of miRNAs 467f and 30a-3p after BD in relation to the level of percentual decrease of myocardial contraction efficiency after 6 h. BD, brain death; miRNA, microRNA.

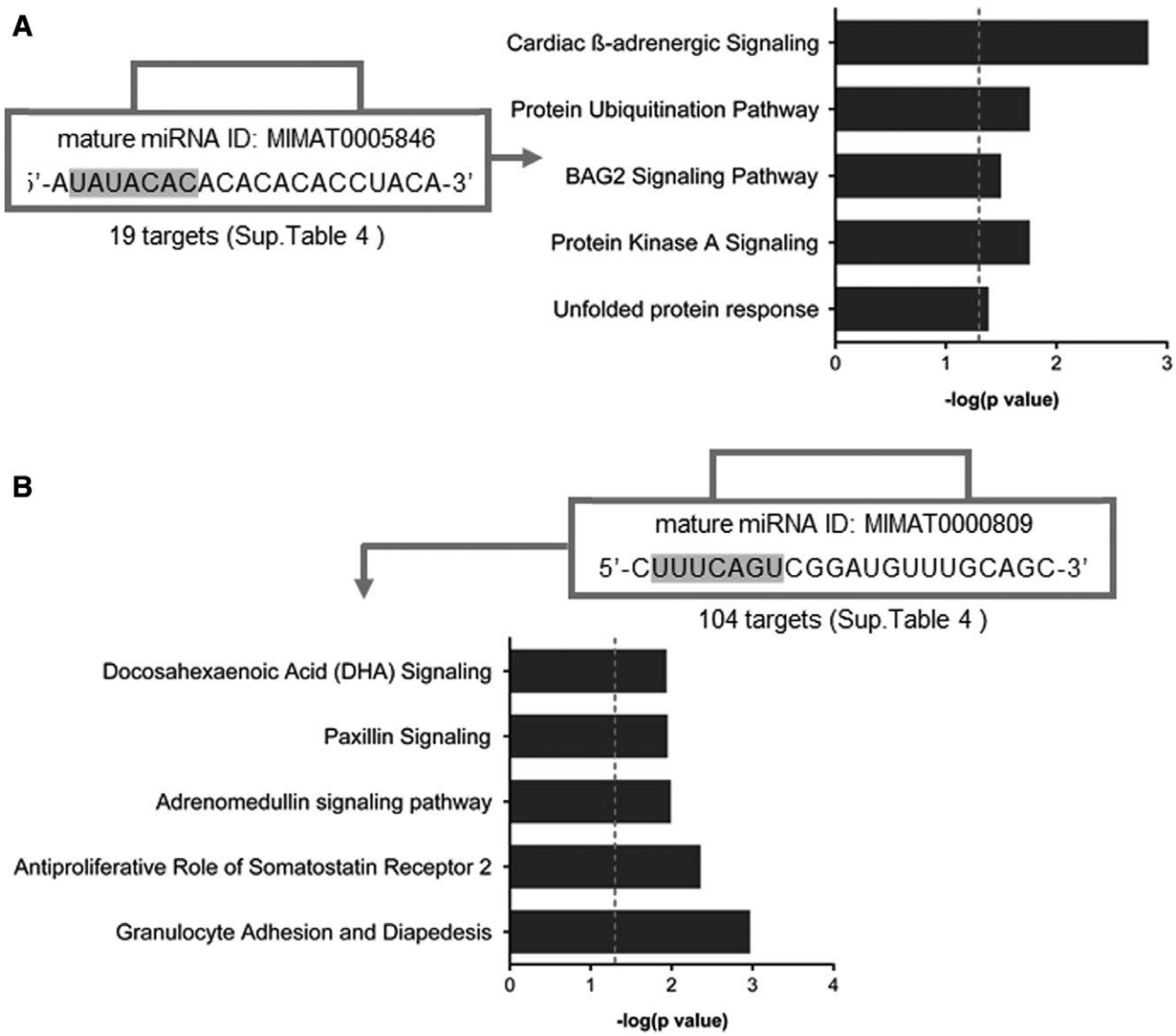

FIGURE 7. Functional pathways enrichment analysis for the DEMs targets of miR-467F (A) and miR-30a-3p (B). The bar charts show the top 5 most enriched pathways for the targets of miR-467F (miRbase ID: MIMAT0005846) and miR-30a-3p (miRbase ID: MIMAT0000809). The sequences of both mature miRNAs are shown with their seed sequence highlighted in gray. BAG2, Bcl2-associated athanogene 2; DEM, differentially expressed miRNA; miRNA, microRNA.

Changes in the miR-467f expression, upregulated in BD, are also related to the *cardiac beta-adrenergic* and *protein kinase A signaling pathways*, whereas miR-207 seems to promote the apoptosis of cardiomyocytes by directly targeting lysosomal-associated membrane protein 2.[19] Among the dysregulated miRNAs identified here after BD, miR-1 family members are the most abundant miRNAs expressed in the heart and seem to be associated with several mechanisms of apoptosis regulation.[6,7,20] In addition, the supplementation of miR-1-3p increased the expression of mitochondrial DNA-encoded proteins in the presence of isoproterenol-induced heart failure in mice, reducing myocardial fibrosis and apoptosis.[21]

In the present study, expression profiles of the miR-30a-3p and miR-467f in the myocardial tissue showed an important correlation with the degree of LV dysfunction after 6 h of BD induction, demonstrating the influence of the *cardiac beta-adrenergic* and apoptotic pathways. Moreover, the preservation of LV function observed with HSS infusion after BD was associated with the reversion of the dysregulated expression of 9 miRNAs related to BD changes, 4 of them directly involved in the amelioration of apoptotic pathways. Besides their relationship with morphological changes, the associations of miRNA expression with the degree of cardiac performance and myocardial reverse remodeling observed here have also been described in several cardiovascular diseases. The expression levels of miR-1-3p have been found to be directly associated with LV performance in models of hypertrophic cardiomyopathy[20] and heart failure.[7,21] Additionally, miR-125b-5p has been recognized as an ischemic stress-responsive protector against cardiomyocyte apoptosis, showing direct correlation with improved myocardial function after experimental infarction in mice.[22]

Other important miRNA alterations currently associated with HSS treatment after BD included DEMs that regulated targets related to several growth factors and homeostasis signaling pathways. Reduction in the expression of miR-197-3p was observed after HSS infusion, which has been associated with improved microcirculation after BD induction.[23] Of interest, downregulation of miR-197-3p normalizes endothelial cell proliferation and migration by targeting insulin-like growth factor type 1 and BCL2 in the presence of vascular endothelial injury,[24] while its upregulation has been associated with a higher risk of venous thromboembolism in patients.[25] MiRNA-467f has been identified as a translational suppressor of thrombospondin-1,[26] and the reversion of its overexpression under HSS administration should potentially decrease a possible angiogenic effect triggered by BD. Other miRNAs activated by HSS were shown to play an unavoidable role in controlling the fibrogenic process and maintaining normal endothelial phenotype. Under high-glucose conditions, miR-200b-3p upregulation appears to protect against endothelial to-mesenchymal transition and to maintain normal endothelial function.[27] Overexpression of miR-30 family is directly associated with the downregulation of connective tissue growth factor, a key profibrotic protein related to structural changes in the extracellular matrix of the myocardium.[6,28]

Primary and late graft dysfunction are major concerns in heart transplantation. Donor heart apoptosis has been associated with early and late allografts failure,[29,30] and recent data have emphasized the importance of donor apoptotic cell therapy as an emerging strategy in promoting transplantation tolerance.[30] Indeed, molecular markers of apoptosis in the hearts obtained from BD donors have been associated with significant myocardial alterations and primary graft dysfunction.[2,5] New therapeutic approaches have been experimentally tested to reduce donor heart apoptosis, resulting in significant recovery of the graft systolic function.[31-33] Moreover, a heart transplant recipient therapy has been analyzed to reverse the donor heart deterioration by suppressing the signaling pathways of inflammation and apoptosis.[34]

Different miRNAs have been identified as biomarkers of ischemic-reperfusion injury alterations[35] and acute or chronic rejection after heart transplantation.[36-38] It has been demonstrated that endothelium-enriched miRNAs can discriminate patients with cardiac allograft vasculopathy.[39] Moreover, the investigation of these biomarkers in patients who underwent coronary angiography confirmed the role of endothelial apoptosis and myocardial fibrosis transformation in the pathogenesis of chronic dysfunction after heart transplantation.[40] As the downregulation of miR-200b-3p, observed here after BD induction, has been associated with the transdifferentiation of the endothelial cells,[12,27] it opens the possibility of the use of this miRNA as a future biomarker for chronic cardiac dysfunction after transplantation.

To our knowledge, this study is the first to discuss the relevance of the identification of miRNAs as biomarkers of cardiac graft deterioration due to BD, demonstrating the association between expression profiles of some miRNAs and the modifications of myocardial systolic function after BD. The finding that the signaling and regulatory pathways modified by these noncoding RNA molecules overlap with the pathophysiological processes previously documented in the same experimental setup[9] and known to occur in hearts from BD donors corroborate a major role for miRNAs in the coordination of these molecular and physiological changes. Moreover, it was also possible to demonstrate the partial reversion of these mechanisms with the use of HSS, validating the previous studies developed by our group in this field.[9,23]

This investigation has limitations related to the small number of studied animals, making it difficult to clearly define the relationship between miRNAs and functional changes. Nonetheless, the wide screening performed in 641 miRNAs aided in the identification of several molecules related to the observed alterations. Although most of the studies with miRNAs have been performed in vitro and in vivo animal models, the fact that these molecules have high-sequence conservation across species indicates also their potential functional redundancies in regulating the same key biologic processes. Furthermore, miRNAs are soluble molecules that can also be detected in blood samples, collaborating to strengthen their clinical impact. The maintenance of prolonged anesthesia with isoflurane in the SHAM group may have induced some miRNAs differential expressions, but this phenomenon is normally related to the expression of different microRNAs than those observed in this study.[41]

Taken together, these findings suggest that the identified miRNAs arise as putative markers of BD donor heart

dysfunction and possible therapeutic targets to be investigated. Further studies are needed to validate these observations in biopsies and in the serum of BD heart donors, opening a perspective to improve the graft quality and to better understand the pathophysiology of BD and its possible influence on early and late cardiac allografts failure.

REFERENCES

1. Tryon D, Hasaniya NW, Jabo B, et al. Effect of left ventricular dysfunction on utilization of donor hearts. *J Heart Lung Transplant.* 2018;37:349–357.
2. Birks EJ, Yacoub MH, Burton PS, et al. Activation of apoptotic and inflammatory pathways in dysfunctional donor hearts. *Transplantation.* 2000;70:1498–1506.
3. Trivedi JR, Cheng A, Gallo M, et al. Predictors of donor heart utilization for transplantation in United States. *Ann Thorac Surg.* 2017;103:1900–1906.
4. Toldo S, Quader M, Salloum FN, et al. Targeting the innate immune response to improve cardiac graft recovery after heart transplantation: implications for the donation after cardiac death. *Int J Mol Sci.* 2016;17:E958.
5. Marasco SF, Sheeran FL, Chaudhuri K, et al. Molecular markers of programmed cell death in donor hearts before transplantation. *J Heart Lung Transplant.* 2014;33:185–193.
6. Chen C, Ponnusamy M, Liu C, et al. MicroRNA as a therapeutic target in cardiac remodeling. *Biomed Res Int.* 2017;2017:1278436.
7. Sucharov CC, Kao DP, Port JD, et al. Myocardial microRNAs associated with reverse remodeling in human heart failure. *JCI Insight.* 2017;2:e89169.
8. Halushka PV, Goodwin AJ, Halushka MK. Opportunities for microRNAs in the Crowded Field of Cardiovascular Biomarkers. *Annu Rev Pathol.* 2019;14:211–238.
9. Magalhães DMS, Zanoni FL, Correia CJ, et al. Hypertonic saline modulates heart function and myocardial inflammatory alterations in brain-dead rats. *J Surg Res.* 2019;235:8–15.
10. Ling Q, Xie H, Li J, et al. Donor graft MicroRNAs: a newly identified player in the development of new-onset diabetes after liver transplantation. *Am J Transplant.* 2017;17:255–264.
11. Roest HP, Ooms LSS, Gillis AJM, et al. Cell-free MicroRNA miR-505-3p in graft preservation fluid is an independent predictor of delayed graft function after kidney transplantation. *Transplantation.* 2019;103:329–335.
12. Glover EK, Jordan N, Sheerin NS, et al. Regulation of endothelial-to-mesenchymal transition by MicroRNAs in chronic allograft dysfunction. *Transplantation.* 2019;103:e64–e73.
13. Tingle SJ, Sewpaul A, Bates L, et al. Dual MicroRNA blockade increases expression of antioxidant protective proteins: implications for ischemia-reperfusion injury. *Transplantation.* 2020;104:1853–1861.
14. Zhou M, Hara H, Dai Y, et al. Circulating organ-specific MicroRNAs serve as biomarkers in organ-specific diseases: implications for organ Allo- and Xeno-transplantation. *Int J Mol Sci.* 2016;17:E1232.
15. Roca-Alonso L, Castellano L, Mills A, et al. Myocardial MiR-30 downregulation triggered by doxorubicin drives alterations in β-adrenergic signaling and enhances apoptosis. *Cell Death Dis.* 2015;6:e1754.
16. Yin Y, Yang C. miRNA-30-3p improves myocardial ischemia via the PTEN/PI3K/AKT signaling pathway. *J Cell Biochem.* 2019;120:17326–17336.
17. Si H, Zhang Y, Song Y, et al. Overexpression of adrenomedullin protects mesenchymal stem cells against hypoxia and serum deprivation-induced apoptosis via the Akt/GSK3β and Bcl-2 signaling pathways. *Int J Mol Med.* 2018;41:3342–3352.
18. Wei H, Vander Heide RS. Heat stress activates AKT via focal adhesion kinase-mediated pathway in neonatal rat ventricular myocytes. *Am J Physiol Heart Circ Physiol.* 2008;295:H561–H568.
19. Xing R, Liu D, Cheng X, et al. MiR-207 inhibits autophagy and promotes apoptosis of cardiomyocytes by directly targeting LAMP2 in type 2 diabetic cardiomyopathy. *Biochem Biophys Res Commun.* 2019;520:27–34.
20. Li M, Chen X, Chen L, et al. MiR-1-3p that correlates with left ventricular function of HCM can serve as a potential target and differentiate HCM from DCM. *J Transl Med.* 2018;16:161.
21. He R, Ding C, Yin P, et al. MiR-1a-3p mitigates isoproterenol-induced heart failure by enhancing the expression of mitochondrial ND1 and COX1. *Exp Cell Res.* 2019;378:87–97.
22. Bayoumi AS, Park KM, Wang Y, et al. A carvedilol-responsive microRNA, miR-125b-5p protects the heart from acute myocardial infarction by repressing pro-apoptotic bak1 and klf13 in cardiomyocytes. *J Mol Cell Cardiol.* 2018;114:72–82.
23. Correia CJ, Armstrong R Jr, Carvalho PO, et al. Hypertonic saline solution reduces microcirculatory dysfunction and inflammation in a Rat model of brain death. *Shock.* 2019;51:495–501.
24. Li Y, Wu X, Gao F, et al. MiR-197-3p regulates endothelial cell proliferation and migration by targeting IGF1R and BCL2 in Kawasaki disease. *Int J Clin Exp Pathol.* 2019;12:4181–4192.
25. Wang X, Sundquist K, Svensson PJ, et al. Association of recurrent venous thromboembolism and circulating microRNAs. *Clin Epigenetics.* 2019;11:28.
26. Bhattacharyya S, Sul K, Krukovets I, et al. Novel tissue-specific mechanism of regulation of angiogenesis and cancer growth in response to hyperglycemia. *J Am Heart Assoc.* 2012;1:e005967.
27. Feng B, Cao Y, Chen S, et al. miR-200b mediates endothelial-to-mesenchymal transition in diabetic cardiomyopathy. *Diabetes.* 2016;65:768–779.
28. Zhang X, Dong S, Jia Q, et al. The microRNA in ventricular remodeling: the MIR-30 family. *Biosci Rep*. 2019;39:BSR20190788.
29. Yang J, Popoola J, Khandwala S, et al. Critical role of donor tissue expression of programmed death ligand-1 in regulating cardiac allograft rejection and vasculopathy. *Circulation.* 2008;117:660–669.
30. Dangi A, Yu S, Luo X. Apoptotic cell-based therapies for promoting transplantation tolerance. *Curr Opin Organ Transplant.* 2018;23:552–558.
31. Korkmaz-Icöz S, Li K, Loganathan S, et al. Brain-dead donor heart conservation with a preservation solution supplemented by a conditioned medium from mesenchymal stem cells improves graft contractility after transplantation. *Am J Transplant.* 2020;20:2847–2856.
32. Yuan X, Teng X, Wang Y, et al. Recipient treatment with acetylcholinesterase inhibitor donepezil attenuates primary graft failure in rats through inhibiting post-transplantational donor heart ischaemia/reperfusion injury. *Eur J Cardiothorac Surg.* 2018;53:400–408.
33. Roset F, Ureña JM, Cotrufo T, et al. Treatment of donor Rat hearts prior to transplantation with FLIP (FADD-Like Interleukin beta-converting enzyme (FLICE)-Like inhibitory protein) in cardioplegic solution decreased apoptosis at thirty minutes post-transplantation and decreased total tyrosine phosphorylation levels. *Ann Transplant.* 2018;23:144–152.
34. Wei J, Chen S, Xue S, et al. Blockade of inflammation and apoptosis pathways by siRNA prolongs cold preservation time and protects donor hearts in a porcine model. *Mol Ther Nucleic Acids.* 2017;9:428–439.
35. Zhou L, Zang G, Zhang G, et al. MicroRNA and mRNA signatures in ischemia reperfusion injury in heart transplantation. *PLoS One.* 2013;8:e79805.
36. Heggermont WA, Delrue L, Dierickx K, et al. Low MicroRNA-126 levels in right ventricular endomyocardial biopsies coincide with cardiac allograft vasculopathy in heart transplant patients. *Transplant Direct.* 2020;6:e549.
37. Sukma Dewi I, Hollander Z, Lam KK, et al. Association of serum MiR-142-3p and MiR-101-3p levels with acute cellular rejection after heart transplantation. *PLoS One.* 2017;12:e0170842.
38. Mas VR, Dumur CI, Scian MJ, et al. MicroRNAs as biomarkers in solid organ transplantation. *Am J Transplant.* 2013;13:11–19.
39. Singh N, Heggermont W, Fieuws S, et al. Endothelium-enriched microRNAs as diagnostic biomarkers for cardiac allograft vasculopathy. *J Heart Lung Transplant.* 2015;34:1376–1384.
40. Almufleh A, Zhang L, Mielniczuk LM, et al. Biomarker discovery in cardiac allograft vasculopathy using targeted aptamer proteomics. *Clin Transplant.* 2020;34:e13765.
41. Chen Y, Zhou ZF, Wang Y. Prediction and analysis of weighted genes in isoflurane induced general anesthesia based on network analysis. *Int J Neurosci.* 2020;130:610–620.